Research Article | Vol. 28, No. 14 / 6 July 2020 / Optics Express 20489
Optics EXPRESS

Characterization of nanoscale gratings by spectroscopic reflectometry in the extreme ultraviolet with a stand-alone setup

LUKAS BAHRENBERG,[1,2,*] SERHIY DANYLYUK,[3] SVEN GLABISCH,[1,2] MOEIN GHAFOORI,[1,2] SOPHIA SCHRÖDER,[1,2] SASCHA BROSE,[1,2] JOCHEN STOLLENWERK,[1,2,3] AND PETER LOOSEN[1,2,3]

[1]RWTH Aachen University TOS - Chair for Technology of Optical Systems, 52074 Aachen, Germany
[2]JARA - Fundamentals of Future Information Technology, 52425 Jülich, Germany
[3]Fraunhofer ILT - Institute for Laser Technology, 52074 Aachen, Germany
[*]lukas.bahrenberg@tos.rwth-aachen.de

Abstract: The authors present a study on the dimensional characterization of nanoscale line gratings by spectroscopic reflectometry in the extreme ultraviolet spectral range (5 nm to 20 nm wavelength). The investigated grating parameters include the line height, the line width, the sidewall angle and corner radii. The study demonstrates that the utilization of shorter wavelengths in state-of-the-art optical scatterometry provides a high sensitivity with respect to the geometrical dimensions of nanoscale gratings. Measurable contrasts are demonstrated for dimensional variations in the sub-percent regime, down to one tenth of a nanometer and one tenth of a degree in absolute terms. In an experimental validation of the method, it is shown that reflectance curves can be obtained in a stand-alone setup using the broadband emission of a discharge produced plasma as the source of EUV radiation, demonstrating the potential scalability of the method for industrial uses. Simulated reflectance curves are fit to the experimental curves by variation of the grating parameters using rigorous electromagnetic modeling. The obtained grating parameters are cross-checked by a scanning electron microscopy analysis.

1. Introduction

The characterization of nanoscale gratings plays an important role in metrology for semiconductor manufacturing [1]. One of the most widely used metrology methods employed today for it is scatterometry. Scatterometry encompasses a range of optical metrology methods including reflectometry and ellipsometry, which employ light from the deep ultraviolet to the infrared as the probing radiation [1]. These methods are able to deliver signature signal curves of the grating under investigation, as a function of wavelength or incidence angle and over a target area smaller than $100 \times 100\ \mu m^2$. The signal curves are characteristic of the geometry and the material of a nanoscale grating. However, they do not translate directly into the grating parameters of interest. Instead, a physical model is necessary to fit simulated signal curves to obtained experimental signal curves, reconstructing the grating parameters [2].

As dimensions in semiconductor manufacturing continue to shrink and the architectures and materials to be investigated become more complex [3], characterizing nanoscale gratings becomes ever more challenging. Although scatterometry in the optical spectral range is already used to successfully characterize nanoscale gratings with pitches below the diffraction limit [2], a further reduction of grating dimensions will lead to a decrease of sensitivity with respect to the exact grating line shape [3]. Further, shrinking the grating dimensions causes the material volume with which the probing radiation interacts to decrease, which similarly leads to a decreasing sensitivity of scatterometry [3]. Apart from that, the optical constants that characterize the grating materials optically are also subject to change when feature sizes approach single-digit

#396001 https://doi.org/10.1364/OE.396001
Journal © 2020 Received 27 Apr 2020; revised 10 Jun 2020; accepted 11 Jun 2020; published 25 Jun 2020

Optics EXPRESS

nanometers, which leads to further uncertainties in the reconstruction of the grating parameters [3]. The mentioned drawbacks that classical scatterometry faces are unlikely to be overcome by incremental improvements of current methods [3].

Therefore, this work investigates the use of the extreme ultraviolet (EUV) spectral range from 5 nm to 20 nm wavelength for the characterization of nanoscale gratings. These smaller wavelengths are of the same order of magnitude as grating dimensions typically investigated nowadays and in the foreseeable future [3]. This leads to an enhanced dependency of diffraction efficiency on the grating line geometry, which allows for an accurate characterization thereof. Besides, a strong light-material interaction is characteristic for this spectral region [4], which can increase the measurement sensitivity with respect to very small material volumes. Further, photons in the EUV interact with bound core electrons rather than with delocalized valence electrons [4]. This stands in contrast to photons in the ultraviolet and visible spectral range and leads to optical constants in the EUV being less dependent on confined dimensions.

Previous promising efforts to employ EUV radiation for the characterization of nanoscale gratings have been undertaken by other research groups based on the analysis of several diffraction orders [5,6]. Other similar efforts deal with the characterization of EUV lithography masks where the gratings have a Bragg type mirror as a substrate [7,8].

In contrast to these studies, the metrology method pursued in this work is not higher diffraction orders scatterometry, but multi-angle spectroscopic reflectometry in the extreme ultraviolet using grazing incidence illumination. This method analyzes only the 0^{th} diffraction order (specular reflectance) for the sake of experimental robustness and accuracy but does so under a multitude of grazing angles, azimuthal orientations of the grating and over a broad spectral range. The method has previously shown its feasibility in the metrology of ultrathin film systems, where EUV radiation has already proven to be beneficial [9,10].

2. Spectroscopic reflectometry in the extreme ultraviolet for nanoscale grating characterization

Similar to existing scatterometry approaches in the optical spectral range, the presented metrology method is an indirect method that needs a physical model of the photon interaction with the grating. In order to interpret measured signal curves adequately and reconstruct the required grating parameters, a recursive fit of a simulated signal curve to the measured one is necessary by varying the grating parameters (see Fig. 1).

The measured signal curves $R(u_i)$ correspond to the reflectance as a function of different illumination parameters u_i, namely the wavelength λ, the polarization state $\vec{J}$, the grazing angle θ and the azimuthal orientation φ. The wavelength stands out as an illumination parameter in this work since the presented method is a spectroscopic one, measuring over a broad spectral range in every single measurement (see section 4). The other illumination parameters can be varied as needed.

The grating geometry is described by the six cross-sectional parameters v_i, defined in Fig. 1: the grating pitch p, the line width w, the line height h, the sidewall angle α and the two corner radii $r_{1,2}$. The line width w is defined at half height of the grating line. In comparison with the traditional top width and bottom width definition, this has the advantage that the cross-sectional area of the grating line remains constant when the sidewall angle α is varied and other parameters are kept constant.

Reflectometry in the extreme ultraviolet, as presented in this work, is based on the approach to measure the reflectance of a nanoscale grating at grazing angles (5° to 15°) over a broad spectral range in the extreme ultraviolet (5 nm to 20 nm wavelength). The grazing angles of illumination are varied with respect to the surface (grazing angle θ) and with respect to the azimuthal orientation (azimuthal angle φ) of the grating lines (see Fig. 1). The grazing angles cannot be arbitrarily large because a sufficient reflectance of the sample has to be maintained in

Optics EXPRESS

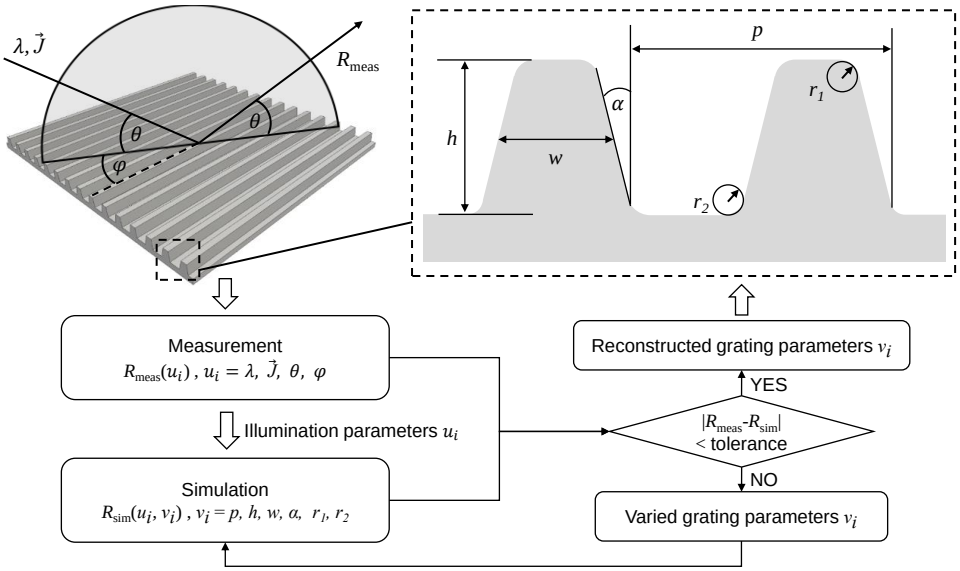

Fig. 1. Schematic representation of recursive model fit for the extraction of nanoscale grating dimensions

order to keep the light flux high and required integration times in practical applications low. As long as the incidence angle is below or not significantly higher than the critical angle of total external reflection [11,4], a high reflectance is assured for all relevant materials.

The reflectance curves (obtained from simulations) of an unstructured substrate and a nanoscale grating of the same material at two grazing incidence angles are shown in Fig. 2. Large differences between a plain and a structured substrate illustrate convincingly that the reflectance contains meaningful information about the grating under investigation.

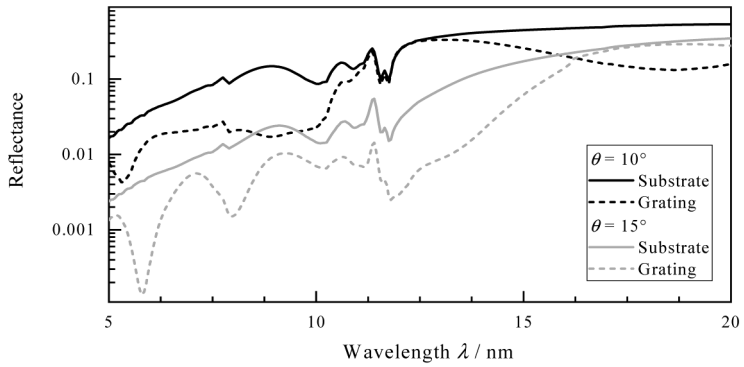

Fig. 2. Reflectance curves (mean of reflectance for s- and p-polarization) obtained from simulations for a fused silica nanoscale grating compared to an unstructured substrate with the same optical constants. The azimuthal angle $\varphi = 0$. The parameters of the grating are defined in Table 1 below (Grating 1).

Even though propagating higher diffraction orders of the grating may exist, measuring only the specular reflectance (0^{th} diffraction order) for the sake of grating characterization and not including higher diffraction orders has significant practical advantages regarding the robustness and feasibility of the method. Firstly, detectors can be placed in a fixed position independently of

Optics EXPRESS

Table 1. Nominal grating parameters used for the sensitivity study

Grating parameter			Grating 1	Grating 2
period	p	(nm)	125	62.5
line width	w	(nm)	50	25
line height	h	(nm)	40	20
sidewall angle	α	(deg)	20	20
corner radius	r_1	(nm)	7	3.5
corner radius	r_2	(nm)	7	3.5

the grating period since the 0^{th} diffraction order beam does not change direction with respect to the illumination. Secondly, a spectrally broadband characterization can easily be conducted in a single measurement with a spectral decomposition of the 0^{th} diffraction order after reflection off the grating. This would be very complicated or even impossible when investigating higher diffraction orders that would exhibit spectral overlaps in the diffraction spectrum. Further, it can be assumed that part of the information contained in higher diffraction orders is, anyway, indirectly encoded in the reflectance because of energy conservation, e.g. maxima in first order diffraction efficiency (as a function of incidence angle or wavelength) often correspond to minima in the reflectance or vice versa. Additionally, in this wavelength range one can conveniently control the number of propagating higher diffraction orders by change of the incidence angle, further increasing the amount of information for the analysis.

3. Sensitivity study for fused silica gratings

The first step to demonstrate the viability of the metrology method presented in this paper is the calculation of the contrasts in the reflectance curves $\delta R(u_i,\ v_i,\ \delta v_i)$ caused by small variations in the grating parameters δv_i. The quantity introduced here to describe these contrasts is the normalized sensitivity s_{norm} [12]:

$$s_{\text{norm}}(u_i, v_i) = \frac{\overbrace{(R(u_i,\ v_i) - R(u_i,\ v_i + \delta v_i))}^{\delta R(u_i, v_i, \delta v_i)}/R(u_i, v_i)}{\delta v_i / v_i} = \frac{\delta R(u_i, v_i,\ \delta v_i)/R(u_i, v_i)}{\delta v_i / v_i}. \tag{1}$$

This quantity states how much the reflectance changes relatively when a certain relative change is applied to one of the grating parameters. It is calculated for s- and p-polarization separately.

The reflectance curves are calculated based on the physics of photon-grating interaction that are fundamentally described by Maxwell's equations. These rigorous electromagnetic simulations are conducted using the software *JCMSuite*, which solves Maxwell's equations based on a finite element method (FEM) [13]. Scatterometry approaches in the optical spectral range perform the modeling mostly based on the rigorous coupled wave analysis (RCWA) [2]. RCWA can usually deliver faster solutions of Maxwell's equations compared to FEM but is not as precise with respect to considering fine structural features in the simulations [14], such as the corner radius investigated in this paper. Therefore, FEM is the simulation technique of choice in this paper. Nevertheless, some reference simulations have been carried out using RCWA in the implementation of the software *Dr.Litho* [15] that cross-validate the results obtained with FEM for gratings without a corner radius.

3.1. Parameter definition and results

For the sensitivity study, a nanoscale line grating is investigated in simulations consisting of fused silica as the sole material. Fused silica as an oxide does not grow oxide layers that would

Optics EXPRESS

complicate the reflectance curves by leading to additional interference effects and by having to account for the optical constants of an additional material. The nominal parameters of the investigated gratings are defined in Table 1.

The utilized optical constants are combined from several sources depending on the wavelength. From 5 nm to 20 nm wavelength, an experimental determination of optical constants was conducted by the authors at a synchrotron on a fused silica substrate of the same material as the gratings in Table 1 (see Fig. 9 in Appendix B). Only in the region around the silicon $L_{2,3}$-absorption edge from approximately 11 nm to 13 nm, values from the literature [16] were used that have a finer wavelength spacing but otherwise agree well with the authors' results in this range. For wavelengths from 20 nm to 40 nm, the values were taken from [4] and for wavelengths from 40 nm to 800 nm from [17]. This combination of optical constants is used throughout this paper.

To calculate the normalized sensitivity, the grating parameters are varied by a small value δv_i of 0.1 nm or 0.1°, respectively. Subsequently, a normalization according to Eq. (1) is conducted, yielding $s_{\mathrm{norm}}(v_i)$. The illumination conditions u_i are set to grazing angles with sufficiently high EUV reflectance (~10°) that are similar to the ones typically used in ellipsometry in the optical spectral range [18]. This makes it possible to directly compare the EUV spectral range to the optical spectral range. Figure 3 shows the results for the normalized sensitivity (see Eq. (1)) for the grating line width w.

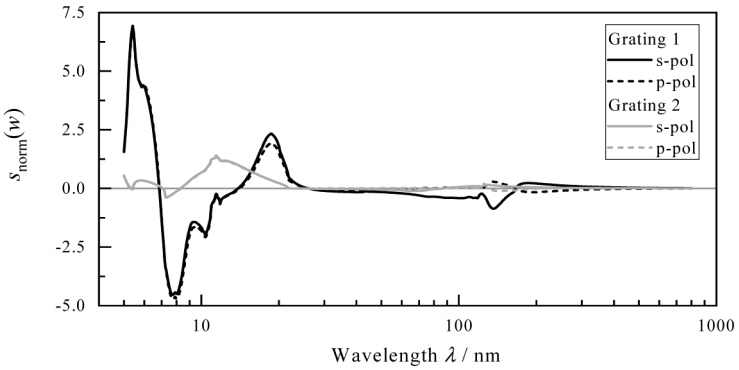

Fig. 3. Normalized sensitivity from the EUV to the visible spectral range for the grating line width w for a grazing angle θ of 10° and an azimuthal orientation φ of 0° (full conical mounting).The curves for two polarizations for Grating 2 look nearly identical except in the 100 nm to 200 nm region.

The results shown in Fig. 3 demonstrate that the normalized sensitivity for the grating line width is significantly higher in the EUV range than it is for wavelengths in the ultraviolet and visible range. This is true for Grating 1 with a linewidth of 50 nm as well as for the scaled-down Grating 2 with a linewidth of 25 nm. The sensitivity values for Grating 2 with the smaller structures are expectedly lower, but maximal in the EUV spectral range.

Qualitatively, very similar results are found for the sensitivity for the other grating parameters defined above (see Figs. 7 and 8 in Appendix A). One difference is that for the sensitivity for the line height, polarization starts to play a role in the EUV spectral range. Further, it appears to be beneficial to increase the grazing angle θ. The sensitivity for a grazing angle of 15° is higher than for 10° for most parameters except the sidewall angle α. The practical downside is, however, the decreasing reflectance that leads to a decreasing light flux in a measurement and longer integration times, accordingly. The variation of the azimuthal orientation φ seems to have little or no benefits with respect to the sensitivity.

Optics EXPRESS

Quantitatively, the sensitivity with respect to the grating parameters is the highest for h and the lowest for the corner radii $r_{1,2}$. These quantitative results are interpreted in the following section, where their translation into the accuracies of grating parameter reconstruction is analyzed.

3.2. Grating parameter accuracy

In practical applications of the metrology method, the quantities of interest are the relative accuracy $\sigma_{v_i,\mathrm{rel}}$ (see Eq. (2)) and the absolute accuracy $\sigma_{v_i,\mathrm{abs}}$ (see Eq. (3)) indicating how accurate a grating parameter v_i can be reconstructed from the acquired signal curves. They are calculated by dividing the accuracy on the measured reflectance $\sigma_R(u_i)$ by the above introduced normalized sensitivity $s_{\mathrm{norm}}(u_i, v_i)$:

$$\sigma_{v_i,\mathrm{rel}}(u_i, v_i) = \frac{\sigma_R(u_i)}{|s_{\mathrm{norm}}(u_i, v_i)|}, \tag{2}$$

$$\sigma_{v_i,\mathrm{abs}}(u_i, v_i) = \frac{\sigma_R(u_i)}{|s_{\mathrm{norm}}(u_i, v_i)|} v_i. \tag{3}$$

The better the accuracy (lower values) on the reflectance σ_R gets and the higher the normalized sensitivity becomes, the better the relative as well as the absolute accuracy (lower values) on the extracted grating parameter will be.

A reflectance accuracy $\sigma_R(u_i)$ of 2% is assumed, a value that is an order of magnitude larger compared to accuracies in synchrotron facilities reaching ~ 0.1% [19]. This choice is made, however, to account for current possibilities in stand-alone setups and is based on the authors' experience in this field [20]. Given this accuracy and normalized sensitivities from Figs. 7 and 8, one can derive accuracies for the grating parameters w, h, α and $r_{1,2}$. Table 2 summarizes the peak sensitivities and corresponding relative and absolute accuracies in the spectral range from 10 nm to 15 nm, the spectral range accessible in the stand-alone setup.

Table 2. Summarized results of the sensitivity study in the spectral range from 10 nm to 15 nm for Gratings 1 and 2

		Grating 1			Grating 2		
Grating parameter		$\lvert s_{\mathrm{norm}}\rvert$[a]	$\sigma_{v_i,\mathrm{rel}}$[b] (%)	$\sigma_{v_i,\mathrm{abs}}$[b] (nm or deg)	$\lvert s_{\mathrm{norm}}\rvert$[a]	$\sigma_{v_i,\mathrm{rel}}$[b] (%)	$\sigma_{v_i,\mathrm{abs}}$[b] (nm or deg)
line width	w	8.0	0.25	0.13	1.30	1.54	0.39
line height	h	20	0.10	0.04	1.40	1.42	0.28
sidewall angle	α	1.0	2.0	0.40	0.25	8.00	1.60
corner radius	r_1	0.2	10	0.70	0.02	100	3.50
corner radius	r_2	0.1	20	1.40	0.01	200	7.00

[a]All values for the normalized sensitivity s_{norm} are approximate and taken from Figs. 7 and 8.
[b]Both accuracies are calculated according to Eqs. (2) and (3) based on the 2% reflectance accuracy.

For the line width w and the line height h, a relative accuracy $\sigma_{v_i,\mathrm{rel}}$ (see Eq. (2)) below 1% is reached for Grating 1. For Grating 2 the relative accuracy is about an order of magnitude worse. In both cases, however, this still corresponds to an absolute accuracy $\sigma_{v_i,\mathrm{abs}}$ (see Eq. (3)) well below 1 nm. The relative accuracy for the side wall angle α is at several percent for both Grating 1 and 2. This corresponds to absolute accuracies around 1° for both gratings. The relative accuracy for the corner radii $r_{1,2}$ is at tens of percents for Grating 1 and at unity or above for Grating 2. This corresponds to an absolute accuracy of around 1 nm for Grating 1 and several nanometers for Grating 2. The accuracy results for the corner radii, however, is affected by the low absolute values of the corner radii, especially for the Grating 2.

Optics EXPRESS

4. Experimental validation of the metrology method

In the second step to demonstrate the viability of the metrology method, EUV reflectance curves are experimentally acquired with a stand-alone setup. Unlike similar measurements carried out at large scale synchrotron facilities [6], carrying out the measurements in a stand-alone setup proves that the method can provide a level of scalability that is important for industrial applications, such as in-line process control for semiconductor manufacturing.

The experimental setup in this paper (see Fig. 4) is based on a discharge produced plasma as the source of unpolarized EUV radiation [21]. The EUV radiation from the source is monitored by two spectrographs that monitor the emission spectrum before and after reflection off of the sample under investigation. The first diffraction grating splits the EUV beam into the first diffraction order that is detected as the source spectrum and the zeroth diffraction order that is focused onto the sample. If a calibration measurement of a sample with known reflectance is carried out additionally to account for all wavelength-dependent photon losses within the experimental setup, the absolute reflectance of the sample can be extracted [22]. The setup has previously been presented in works that encompass the characterization of thin film systems [10] but has undergone some technical changes since in order to improve its accuracy [20].

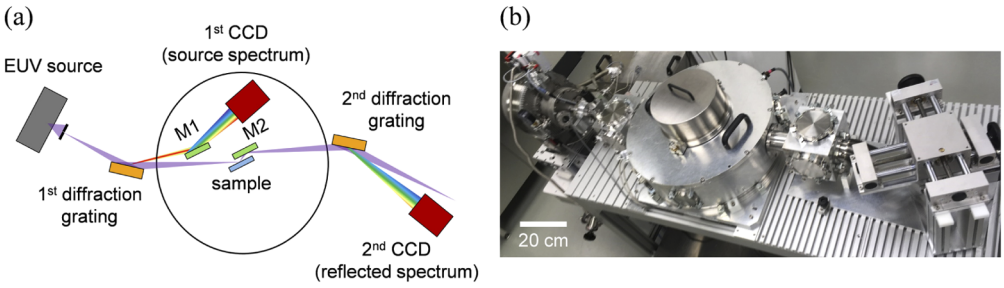

Fig. 4. Stand-alone broadband EUV reflectometry setup. (a) Schematic depiction of the stand-alone setup and its components and (b) photograph of the setup. M1 and M2 are deflection mirrors used to redirect the beam.

A fused silica nanoscale grating (grating area of 15×15 mm^2) like the one investigated in the sensitivity study above, is measured in the setup (fabricated by *EULITHA* with *PHABLE exposure technology*). Its spectroscopic reflectance is measured at different grazing angles θ and azimuthal orientations φ (see Fig. 1 for definitions). The spectral range covered goes from 10.7 nm to 15 nm, a range where a reflectance accuracy of 2% is obtainable with the setup.

The accuracy is estimated from a repeated set of measurements of the same sample after independent alignments. Therefore the accuracy includes noise effects induced during the detection of the spectra as well as uncertainties in incidence angle coming from the alignment of the sample. Further offsets in incidence angle are determined to be $< 0.05°$ in a beam triangulation using reflection off the sample. Offsets in wavelength are determined to be < 10 pm due to the sharp nature of the spectra produced by the discharge EUV source and the fine wavelength digitization (< 10 pm) by the CCD camera pixels [20].

The illumination spot on the sample under normal incidence is ~ 50 µm in the plane of incidence [20] and ~ 3 mm in the direction perpendicular to the plane of incidence. Previous work, however, has shown a successful reduction of spot size in both directions in the same setup [23]. The angular divergence of illumination does not exceed $\pm 0.1°$, for which simulations have shown that this has a negligible effect on the resulting reflectance for this work. This is due to the incidence angle variation having an effect on the reflectance being either within the estimated uncertainty of 2% or a cancellation of the effect within the uncertainty that opposing marginal rays have on the reflectance.

Optics EXPRESS

To measure a reflectance curve at a specific incidence angle, a total of 100 spectra is accumulated on both CCD cameras synchronously and subsequently averaged. Each spectrum is recorded over an integration time of 20 ms and a background spectrum with the same integration time is subtracted from it.

The resulting reflectance curves are shown in Fig. 5 alongside a best fit curve. The fits were obtained with a least squares regression using simulated reflectance curves corresponding to a pre-defined grid of grating parameters. The simulated reflectance curves were obtained with the rigorous FEM modeling technique, described in section 3. The grating parameters of the best fit curve are summarized in Table 3.

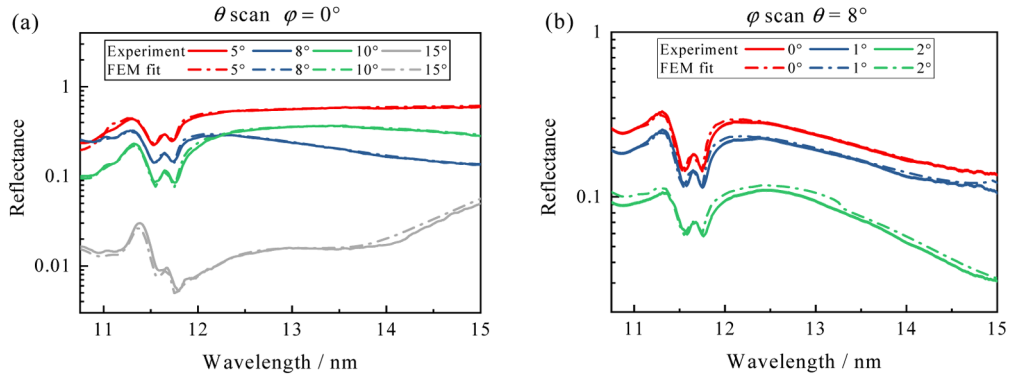

Fig. 5. EUV reflectance curves measured (solid lines) in the stand alone setup and corresponding fits conducted with rigorous finite element method (dashed lines). (a) Experimental scan of the grazing angle θ and (b) experimental scan of the azimuthal orientation φ. The relative reflectance accuracy of 2% is indicated by a band around the reflectance curve (appears very small).

Table 3. Comparison of extracted grating parameters

Grating parameter			FEM fit	SEM characterization
line width	w	(nm)	53.1	(50.0±2.5)
line height	h	(nm)	40.6	(39.0±1.0)
sidewall angle	α	(deg)	15.5	(18.0±2.5)
corner radius	r_1	(nm)	4.3	(7.0±3.0)
corner radius	r_2	(nm)	4.3	(7.0±3.0)

The fits are in agreement with the experimental curves and their indicated uncertainty bands over large parts of the curves. This validates that the FEM model works as intended. Furthermore, it demonstrates that the proposed metrology method can be implemented in a stand-alone setup delivering reflectance curves with sufficient accuracy, exhibiting every important feature when compared to the simulations.

An independent characterization of the nanoscale grating is conducted by means of scanning electron microscopy (SEM). A top down image (Fig. 6(a)) of the grating and a cross-sectional image (Fig. 6(b)) is taken. The grating dimensions are analyzed in these images averaging over a number of grating lines and estimating maximum and minimum values to account for a biased image analysis. Subsequently, a mean value and an uncertainty are derived for each parameter.

Table 3 compares the results of the independently conducted SEM characterization with the FEM fit that is conducted with respect to the measured reflectance curves. The period is not included as a separate parameter since it is a well-controlled parameter in the fabrication of a

Optics EXPRESS

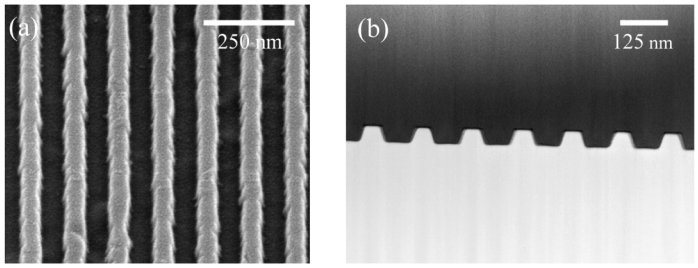

Fig. 6. Scanning electron microscopy analysis of the fused silica grating used for the experimental investigation with (a) a top-down SEM image of the grating and (b) a scanning transmission electron microscopy (STEM) image of the grating cross section.

periodic grating and usually not a parameter of interest in respective metrology. It becomes clear that the values for the FEM fit shown in Table 3 are not in full agreement with the SEM analysis. An obvious reason is that the fit curves do not completely agree with the measured reflectance curves within their respective measurement accuracy. The reasons for this may be on the experimental side and on the modeling side.

On the experimental side, sample-related systematic errors in the measured absolute reflectance may have occurred. One possible source currently under investigation could be a difference in stray light levels caused by a different roughness of a calibration sample and a measured sample. Additionally, the build-up of hydrocarbon contamination of the surface in the setup cannot be ruled out.

On the modeling side, two aspects are named as possible reasons. Despite the author's best efforts, the accuracy of the constructed refractive index database for fused silica may be not high enough. Secondly, the FEM model is not taking into account surface and line edge roughness, both contributing to non-specular energy loss. Accounting for roughness is not always essential to yield satisfying fits for nanoscale grating diffraction efficiency in the EUV spectral range [24]. It depends, however, on the specific grating under investigation and there are examples where roughness plays a crucial role [25,26].

5. Conclusion

In conclusion, it has been demonstrated that EUV radiation offers promising advantages with respect to the dimensional characterization of nanoscale gratings when compared to the optical spectral range used in state-of-the art scatterometry methods.

In a sensitivity study it has been shown that spectroscopic reflectometry in the extreme ultraviolet reveals parameter variations of nanoscale line gratings in the deep sub-nanometer regime down to one tenth of a nanometer and even below if a sufficient measurement accuracy is guaranteed. In relative terms, a grating parameter accuracy for the line height and the line width of well below 1% is obtained when a measurement accuracy of around 2% is maintained. The sidewall angle can be determined with an accuracy of several percent. Corner radii can be determined with an accuracy of tens of percents. Improving the measurement accuracy to below 1% would further improve the reconstruction accuracy.

A comparison with reflectance curves in the optical spectral range demonstrates that EUV reflectance curves are much more sensitive with respect to changes in all of the investigated nanoscale grating parameters.

Experimentally, it has been shown that the metrology method can be implemented in a stand-alone setup that is able to conduct the required measurements of spectroscopic EUV reflectance as a function of incidence angle. The stand-alone setup measures EUV reflectance

Optics EXPRESS

with an accuracy of 2% in the spectral range from approximately 10 nm to 15 nm. Model fits yielding a good agreement with the experimental curves demonstrate the viability of the method and validate it in an experiment. Further, the implementation in a stand-alone setup proves the potential scalability of the method for industrial purposes.

6. Outlook

Future works will include improved modeling containing an updated database for optical constants and an evaluation of surface and line edge roughness. Roughness is deemed to be of importance for EUV reflectance at shallow incidence angles [25]. Once the model fits are brought into full agreement with the experimental curves, the next step will be a comprehensive uncertainty analysis of the reconstructed grating parameters. Beyond considering the experimental uncertainties, it will include the uncertainty in the utilized optical constants, which, as mentioned above, are also determined experimentally.

In order to gain a deeper understanding of the viability of the method with respect to applications in semiconductor-related metrology, it will be essential to include the analysis of cross-correlations between grating parameters in the form of correlation matrices, as was recently performed for thin film analysis [27]. The current expectation is, however, that including different illumination parameters in the reconstruction will allow to minimize the influence of cross-correlations on reconstruction accuracy.

With respect to the types of investigated gratings, future studies will include more complex grating structures with three-dimensional features, addressing important development trends in the semiconductor industry [28]. This may also include features hidden below the grating surface and gratings hidden below the sample surface. In these cases a tunable penetration depth will play an important role in optimizing the final sensitivity in the EUV spectral range.

Appendix A: sensitivity study

Optics EXPRESS

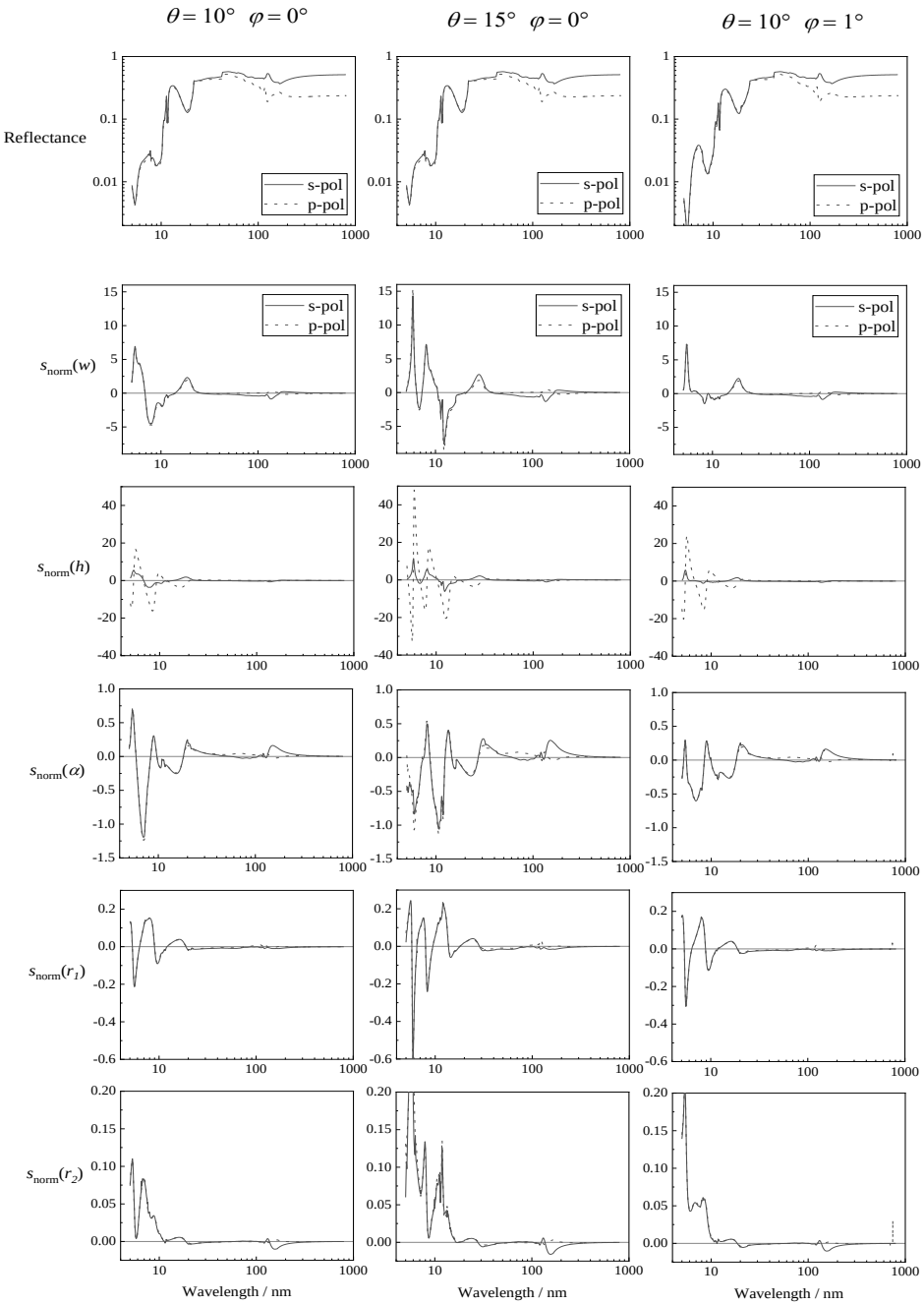

Fig. 7. Reflectance and normalized sensitivity for three different illumination conditions (columns) for the investigated grating parameters of Grating 1 with a period of 125 nm (defined in Table 1). Solid lines show the results for s-polarization and dashed lines for p-polarization.

Optics EXPRESS

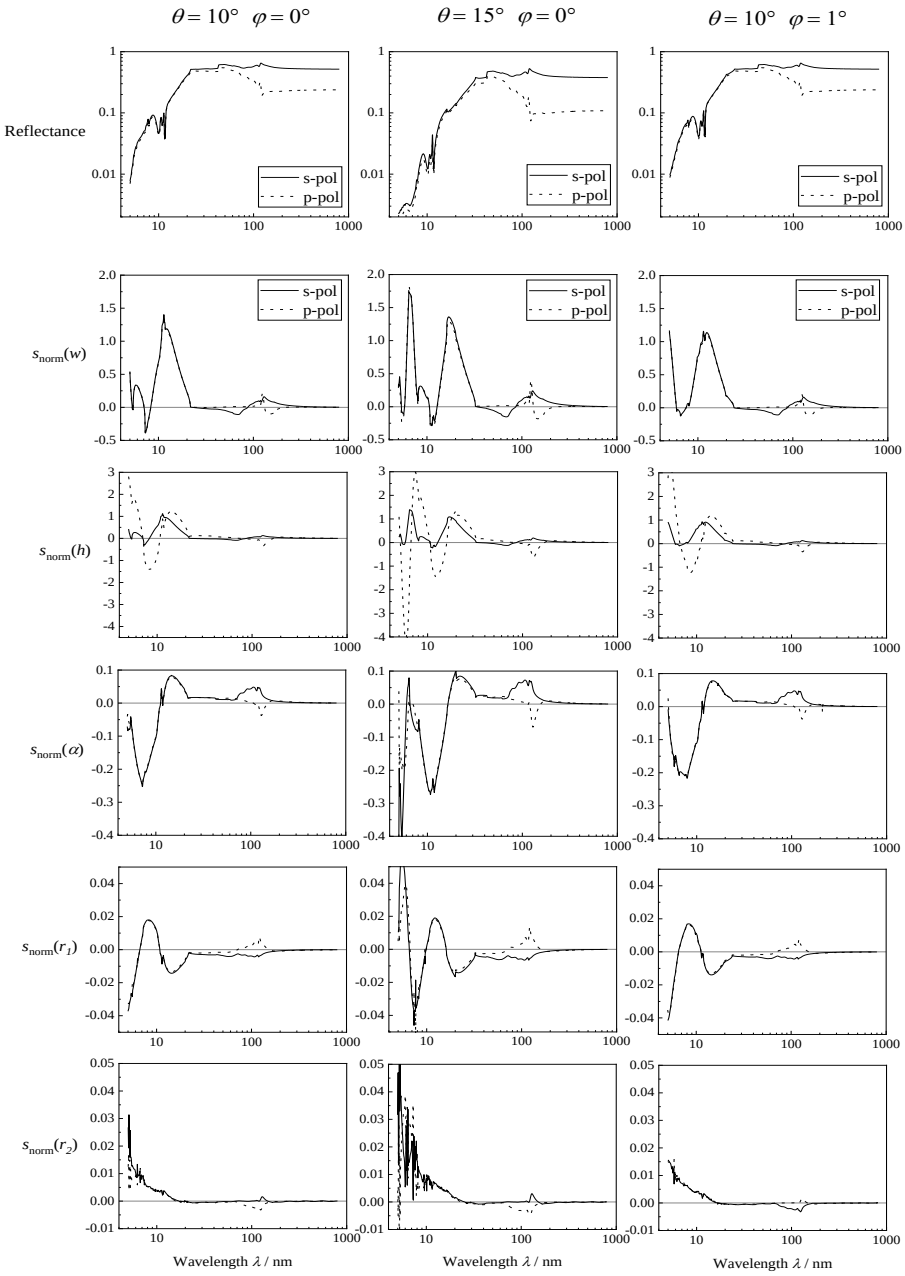

Fig. 8. Reflectance and normalized sensitivity for three different illumination conditions (columns) for the investigated grating parameters of Grating 2 with a period of 62.5 nm (defined in Table 1). Solid lines show the results for s-polarization and dashed lines for p-polarization.

Optics EXPRESS

Appendix B: optical constants

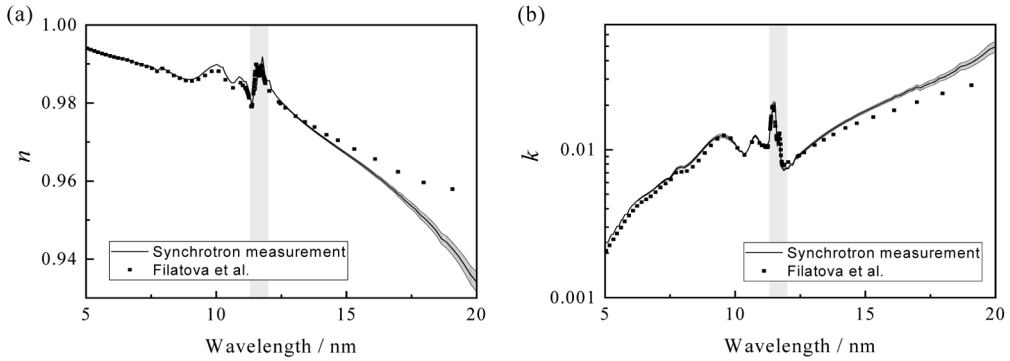

Fig. 9. Optical constants with the values for n (a) and k (b) determined in a synchrotron measurement (conducted at BEAR beamline at ELETTRA synchrotron in Trieste, Italy [29]) and compared to values from Filatova et al. [16]. The highlighted spectral range shows where values were taken from [16] instead of from the synchrotron measurement because of the finer wavelength spacing.

Funding

Deutsche Forschungsgemeinschaft (415848294); Electronic Components and Systems for European Leadership (783247).

Acknowledgments

The authors thank Bernhard Lüttgenau of RWTH Aachen University and Elmar Neumann as well as his colleagues at Helmholtz Nanoelectronic Facility at Research Center Jülich [30] for the SEM characterizations. Furthermore, the authors would like to acknowledge Frank Scholze and Victor Soltwisch of Physikalisch-Technische Bundesanstalt (PTB) for providing reference measurements of samples that helped to calibrate and benchmark the stand-alone setup used in this work. This project has received funding from the Electronic Component Systems for European Leadership Undertaking under grant agreement number 783247 (TAPES3). This Joint Undertaking receives support from the European Union's Horizon 2020 research and innovation programme and Netherlands, France, Belgium, Germany, Czech Republic, Austria, Hungary, Israel.

Disclosures

The authors declare no conflicts of interest.

References

1. A. C. Diebold, A. Antonelli, and N. Keller, "Perspective: Optical measurement of feature dimensions and shapes by scatterometry," APL Mater. **6**(5), 058201 (2018).
2. M. H. Madsen and P.-E. Hansen, "Scatterometry—fast and robust measurements of nano-textured surfaces," Surf. Topogr.: Metrol. Prop. **4**(2), 023003 (2016).
3. B. Bunday, T. A. Germer, V. Vartanian, A. Cordes, A. Cepler, and C. Settens, "Gaps analysis for CD metrology beyond the 22 nm node," Proc. SPIE **8681**, 86813B (2013).
4. B. L. Henke, E. M. Gullikson, and J. C. Davis, "X-ray interactions: photoabsorption, scattering, transmission, and reflection at E=50-30000 eV, Z=1-92," At. Data Nucl. Data Tables **54**(2), 181–342 (1993).
5. Y.-S. Ku, C.-L. Yeh, Y.-C. Chen, C.-W. Lo, W.-T. Wang, and M.-C. Chen, "EUV scatterometer with a high-harmonic-generation EUV source," Opt. Express **24**(24), 28014–28025 (2016).

Optics EXPRESS

6. V. Soltwisch, C. Laubis, A. Fernández Herrero, M. Pflüger, A. Haase, and F. Scholze, "Investigating surface structures by EUV scattering," Proc. SPIE **10143**, 101430P (2017).
7. H. Gross, A. Rathsfeld, F. Scholze, and M. Bär, "Profile reconstruction in extreme ultraviolet (EUV) scatterometry. Modeling and uncertainty estimates," Meas. Sci. Technol. **20**(10), 105102 (2009).
8. P. Ansuinelli, W. M. J. Coene, and H. P. Urbach, "Automatic feature selection in EUV scatterometry," Appl. Opt. **58**(22), 5916–5923 (2019).
9. M. Banyay, L. Juschkin, E. Bersch, D. Franca, M. Liehr, and A. Diebold, "Cross characterization of ultrathin interlayers in HfO2 high-k stacks by angle resolved x-ray photoelectron spectroscopy, medium energy ion scattering, and grazing incidence extreme ultraviolet reflectometry," J. Vac. Sci. Technol., A **30**(4), 041506 (2012).
10. S. Danylyuk, S. Herbert, P. Loosen, R. Lebert, A. Schäfer, J. Schubert, M. Tryus, and L. Juschkin, "Multi-Angle Spectroscopic Extreme Ultraviolet Reflectometry for Analysis of Thin Films and Interfaces," Phys. Status Solidi C **12**(3), 318–322 (2015).
11. D. T. Attwood, A. Sakdinawat, and L. Geniesse, *X-rays and extreme ultraviolet radiation. Principles and applications*, Second edition (Cambridge University, 2016).
12. R. Silver, T. Germer, R. Attota, B. Barnes, and B. Bunday, "Fundamental limits of optical critical dimension metrology: a simulation study," Proc. SPIE **6518**, 65180U (2007).
13. J. Pomplun, S. Burger, L. Zschiedrich, and F. Schmidt, "Adaptive finite element method for simulation of optical nano structures," Phys. Status Solidi B **244**(10), 3419–3434 (2007).
14. T. Fuehner, T. Schnattinger, G. Ardelean, and A. Erdmann, "Dr.LiTHO – A Development and Research Lithography Simulator," Proc. SPIE **6520**, 65203F (2007).
15. S. Burger, L. Zschiedrich, F. Schmidt, P. Evanschitzky, and A. Erdmann, "Benchmark of rigorous methods for electromagnetic field simulations," Proc. SPIE **7122**, 71221S (2008).
16. E. O. Filatova, V. Lukanyov, R. Barchewitz, J.-M. André, M. Idir, and P. Stemmler, "Optical constants of amorphous SiO2 for photons in the range of 60-3000 eV," J. Phys.: Condens. Matter **11**(16), 3355–3370 (1999).
17. E. D. Palik, *Handbook of optical constants of solids*, (Academic, 1985).
18. R. Radoi and C. Flueraru, "Determination of the best incidence angle for ellipsometric measurements," in *Proceedings of IEEE Conference on International Semiconductor Conference* (IEEE, 1998), pp. 245–248.
19. F. Scholze, J. Tümmler, and G. Ulm, "High-accuracy radiometry in the EUV range at the PTB soft x-ray beamline," Metrologia **40**(1), S224–S228 (2003).
20. L. Bahrenberg, S. Glabisch, S. Danylyuk, M. Ghafoori, S. Schroeder, S. Brose, J. Stollenwerk, and P. Loosen, "Nanoscale grating characterization through EUV spectroscopy aided by machine learning techniques," Proc. SPIE **11325**, 113250X (2020).
21. K. Bergmann, G. Schriever, O. Rosier, M. Müller, W. Neff, and R. Lebert, "Highly repetitive, extreme-ultraviolet radiation source based on a gas-discharge plasma," Appl. Opt. **38**(25), 5413–5417 (1999).
22. L. Bahrenberg, S. Glabisch, M. Ghafoori, S. Brose, S. Danylyuk, J. Stollenwerk, and P. Loosen, "Laboratory-based EUV spectroscopy for the characterization of thin films, membranes and nanostructured surfaces," Proc. SPIE **11147**, 111471X (2019).
23. M. Tryus, S. Herbert, D. Wilson, L. Bahrenberg, S. Danylyuk, and L. Juschkin, "Spatially Resolved Spectroscopic Extreme Ultraviolet Reflectometry for Laboratory Applications," J. Nanosci. Nanotechnol. **19**(1), 562–567 (2019).
24. C. Braig, L. Fritzsch, T. Käsebier, E.-B. Kley, C. Laubis, Y. Liu, F. Scholze, and A. Tünnermann, "An EUV beamsplitter based on conical grazing incidence diffraction," Opt. Express **20**(2), 1825–1838 (2012).
25. V. Rehn, V. O. Jones, J. M. Elson, and J. M. Bennett, "The role of surface topography in predicting scattering at grazing incidence from optical surfaces," Nucl. Instrum. Methods **172**(1-2), 307–314 (1980).
26. H. Gross, M.-A. Henn, S. Heidenreich, A. Rathsfeld, and M. Bär, "Modeling of line roughness and its impact on the diffraction intensities and the reconstructed critical dimensions in scatterometry," Appl. Opt. **51**(30), 7384–7394 (2012).
27. M. Tryus, K. V. Nikolaev, I. A. Makhotkin, J. Schubert, L. Kibkalo, S. Danylyuk, A. Giglia, P. Nicolosi, and L. Juschkin, "Optical and structural characterization of orthorhombic LaLuO3 using extreme ultraviolet reflectometry," Thin Solid Films **680**, 94–101 (2019).
28. B. Bunday, E. Solecky, A. Vaid, A. F. Bello, and X. Dai, "Metrology capabilities and needs for 7 nm and 5 nm logic nodes," Proc. SPIE **10145**, 101450G (2017).
29. L. Pasquali, A. de Luisa, and S. Nannarone, "The UHV Experimental Chamber For Optical Measurements (Reflectivity and Absorption) and Angle Resolved Photoemission of the BEAR Beamline at ELETTRA," AIP Conf. Proc. **705**, 1142–1145 (2004).
30. W. Albrecht, J. Moers, and B. Hermanns, "HNF - Helmholtz Nano Facility," JLSRF **3**, A112 (2017).